



UvA-DARE (Digital Academic Repository)

Genetic basis of cardiac ion channel diseases

Koopmann, T.

Publication date
2008

[Link to publication](#)

Citation for published version (APA):

Koopmann, T. (2008). *Genetic basis of cardiac ion channel diseases*.

General rights

It is not permitted to download or to forward/distribute the text or part of it without the consent of the author(s) and/or copyright holder(s), other than for strictly personal, individual use, unless the work is under an open content license (like Creative Commons).

Disclaimer/Complaints regulations

If you believe that digital publication of certain material infringes any of your rights or (privacy) interests, please let the Library know, stating your reasons. In case of a legitimate complaint, the Library will make the material inaccessible and/or remove it from the website. Please Ask the Library: <https://uba.uva.nl/en/contact>, or a letter to: Library of the University of Amsterdam, Secretariat, Singel 425, 1012 WP Amsterdam, The Netherlands. You will be contacted as soon as possible.

Chapter 6

Sodium channel $\beta 1$ -subunit mutations associated with Brugada syndrome and cardiac conduction disease

Hiroshi Watanabe*, Tamara T. Koopmann*, Solena Le Scouarnec*, Tao Yang, Christiana R. Ingram, Jean-Jacques Schott, Sophie Demolombe, Vincent Probst, Frédéric Anselme, Denis Escande, Ans C.P. Wiesfeld, Arne Pfeufer, Stefan Kääh, H.-Erich Wichmann, Can Hasdemir, Yoshifusa Aizawa, Arthur A.M. Wilde, Dan M. Roden, Connie R. Bezzina

* These authors contributed to this work equally.

J Clin Invest, *in press*

Abstract

Brugada syndrome is a genetic disease associated with sudden cardiac death that is characterized by ventricular fibrillation and right precordial ST-segment elevation on ECG. Loss-of-function mutations in *SCN5A*, which encodes the predominant cardiac sodium channel α -subunit $\text{Na}_v1.5$, can cause Brugada syndrome and cardiac conduction disease. However, *SCN5A* mutations are not detected in a majority of patients with these syndromes, suggesting that other genes can cause or modify presentation in these disorders. Here, we investigated *SCN1B*, encoding the function-modifying sodium channel β 1-subunit, in 282 probands with Brugada syndrome and in 44 patients with conduction disease, none of whom had *SCN5A* mutations. We identified three mutations segregating with arrhythmia in three kindreds. Two of these mutations were located in a newly described alternately processed transcript, β 1B. Both the canonical and alternately processed transcripts were expressed in the human heart and were expressed to a greater degree in Purkinje fibers than in heart muscle, consistent with the clinical presentation of conduction disease. Sodium current was lower when $\text{Na}_v1.5$ was coexpressed with mutant β 1 or β 1B-subunits than when it was coexpressed with WT subunits. These findings implicate *SCN1B* as a disease gene for human arrhythmia susceptibility.

6.1 Introduction

Voltage-gated sodium channels are critical for the generation and propagation of the cardiac action potential,^{1,2} and mutations in *SCN5A*, the gene encoding the major pore-forming sodium channel α -subunit in the heart ($\text{Na}_v1.5$), cause multiple cardiac arrhythmia syndromes.¹⁻⁴ Mutations producing enhanced inward current during the course of the action potential plateau, often as a consequence of destabilized fast inactivation of the channel, cause long QT syndrome type 3 (LQT3, OMIM 603830).^{1,2} On the other hand, a reduction in sodium current leads to cardiac conduction disease, which may be progressive (OMIM 113900),^{1,3} and Brugada syndrome (OMIM 601144), characterized by ST-segment elevation in the right precordial leads (V1 to V3) of the 12-lead electrocardiogram (ECG) and episodes of ventricular fibrillation.⁴ Multiple mechanisms have been described that reduce sodium current in these syndromes, including altered gating of the channel or reduced cell surface expression.⁵ In addition, mutations in *SCN5A* may manifest with an overlap of these different phenotypes.⁶⁻¹⁰ However, mutations in *SCN5A* are found in fewer than 30% of patients with Brugada syndrome, indicating involvement of other genes.¹¹ A mutation in the glycerol-3-phosphate dehydrogenase 1-like gene (*GPD1L*) has recently been reported in a large kindred with Brugada syndrome¹²; however, *GPD1L* mutations are rare in Brugada syndrome.¹³ Antzelevitch et al. have recently reported mutations in the gene encoding the L-type calcium channel (*CACNA1C*) or its β 2b-subunit (*CACNB2*) in Brugada syndrome patients with unusually short QT intervals,¹⁴ but the frequency of these defects as a cause for more-typical Brugada syndrome is unknown. *SCN5A* mutations are also not identified in the majority of patients with cardiac conduction disease.¹⁵

Sodium channels are multi-subunit protein complexes composed not only of pore-forming α -subunits but also of multiple other protein partners including auxiliary function-modifying β -subunits.^{16,17} In humans, four sodium channel β -subunits (β 1 to β 4, encoded by *SCN1B* to *SCN4B*) have been identified, and they share a common predicted protein topology: a large extracellular N-terminal domain (including an immunoglobulin-like domain), a single transmembrane segment, and an intracellular C-terminal domain.¹⁷ Functions attributed to β -subunits include an increase in sodium channel expression at the cell surface, modulation of channel gating and voltage dependence, and a role in cell adhesion and recruitment of cytosolic proteins such as ankyrin G.¹⁷

The β 1 transcript arises from splicing of exons 1-5 of the *SCN1B* gene (Figure 1, A and B). More recently, a second transcript has been described, arising from splicing of exons 1-3 with retention of a segment of intron 3 (termed exon 3A), leading to an alternate 3' sequence (Figure 1, A and B).^{18,19} This latter transcript encodes the β 1B-subunit, which, in spite of the different 3' sequence, has a predicted protein topology similar to that of β 1 (Figure 1C).¹⁹ The β 1B-subunit has been shown to increase a neuronal sodium current ($\text{Na}_v1.2$),¹⁹ but its effects on $\text{Na}_v1.5$ current have not yet been investigated, although β 1 and β 1B are both expressed in heart.^{19,20}

Since loss-of-function $\text{Na}_v1.5$ mutations cause conduction disease and Brugada syndrome, one could envision that mutations in sodium channel β -subunits could also underlie these disorders by decreasing sodium current. Therefore, we tested the hypothesis that mutations in *SCN1B* coding sequences, for either β 1 or β 1B, underlie cases of conduction disease and Brugada syndrome.

6.2 Methods

Study populations

The study populations consisted of (i) unrelated Brugada syndrome probands ascertained at the Academic Medical Center, Amsterdam, the Netherlands (n=38), l'institut du thorax, Nantes, France (n=216), and the Niigata University Graduate School of Medical and Dental Sciences, Niigata, Japan (n=28); and (ii) patients with cardiac conduction disease ascertained at the Academic Medical Center, Amsterdam (n=2), l'institut du thorax, Nantes (n=39), and Ege University School of Medicine, Izmir, Turkey (n=3). The study was performed according to a protocol approved by the local ethics committees. Informed consent was obtained from all patients. Coding region and splice site mutations in *SCN5A* had been previously excluded in all probands by SSCP-DNA sequencing, dHPLC-DNA sequencing, or by direct sequencing using primers in flanking intronic sequences.

Mutation analysis

Probands with Brugada syndrome and cardiac conduction disease were screened for mutations in regions of the *SCN1B* gene encoding $\beta 1$ and $\beta 1B$, except for Japanese probands, who were screened only in the regions of *SCN1B* gene encoding $\beta 1B$. Screening for mutations was performed by PCR amplification of coding regions and flanking intronic sequences, followed by direct sequencing of amplicons on an ABI Prism 3730 DNA Sequence Detection System (Applied Biosystems, Foster City, CA). Primer sequences are listed in Table 1:

Table 1: Sequence of oligonucleotide primers for *SCN1B* screening

Exon	Forward primer	Reverse primer
1	CCTCTCGCGCCGCTATTAATACC	CGTGTCCCGAGCGCCACTC
2	GTGAGGGGTCTGGCATTGCT	TCCAGGTCAGCAATCACAGCAT
3	GGGTCAGGTAAGGGAAGAGAGG	TGTCCCTCCATCTGGCTCTC
4	CCCAGGGAGGTTGAGCCACT	CCTCTCTGGCAAGTGTGACGG
5	ACCGCTACCTTCCCCCATCC	GACTTCGGCCCC TCCAATC
3A	GTCTACCGCTGCTCTTCTCG	CAGGCGTGTGCCTGCAGCTG

Control populations

We screened randomly selected and unrelated Dutch Caucasian individuals (n=176), Caucasian individuals (n=702) selected from the KORA S4 survey, which included population-based southern German individuals (n=4,261) surveyed between 1999 and 2001,²¹ unrelated Turkish Caucasian individuals (n=150), and four different ethnic groups (Caucasian, African-American, Hispanic, Asian, n=94 for each group) from the Coriell Cell Repositories (Camden, NJ). The Coriell samples were resequenced as described above by the J. Craig Venter Institute through the NHLBI Resequencing and Genotyping Program. The other control samples were genotyped at the identified mutation sites.

Subunit mRNA abundances in human cardiac tissue

Real-time RT-PCR was used to quantify subunit abundances. Assays were conducted in non-diseased human hearts obtained from the University of Szeged, that were technically unusable for transplantation based on logistic considerations.²² Before cardiac explantation, organ donor patients did not receive medication except dobutamine, furosemide and plasma expanders. The investigations conformed to the principles outlined in the Helsinki Declaration of the World Medical Association. All experimental protocols were approved by the Ethical Review Board of the Medical Center of the University of Szeged (No. 51-57/1997 OEJ). The left ventricles from 6 donors and the right ventricles from 6 donors were dissected and stored in cardioplegic solution at 4°C for 4~8 h before being frozen in liquid nitrogen. Purkinje fiber mRNA was extracted from false tendons dissected from the ventricles of 6 donors. Further information on the donors is presented in Table 2:

Table 2: Characteristics of non-diseased donors

Subject No.	Gender	Age (years)	Tissues
1	Female	65	LV, RV
2	Female	49	LV, RV
3	Female	41	LV, RV
4	Female	35	LV, RV
5	Male	43	LV
6	Male	42	LV
7	Male	38	RV
8	Female	18	RV
9	Male	18	Purkinje
10	Male	20	Purkinje
11	Female	46	Purkinje
12	Female	49	Purkinje
13	Female	28	Purkinje
14	Female	65	Purkinje

LV, left ventricle; RV, right ventricle

Total RNA from each cardiac sample was isolated and DNase-treated with the RNeasy Fibrous Tissue Mini Kit (Qiagen) following the manufacturer's instructions. The quality of total RNA was assessed with polyacrylamide-gel micro-electrophoresis (2100 Bioanalyzer). Absence of genomic DNA contamination was verified by PCR. First-strand cDNA was synthesized from 2 µg total RNA with High-Capacity cDNA Archive Kit (Applied Biosystems). Real-time PCR was performed on a Taqman system with pre-designed 6-carboxyfluorescein (FAM-labeled) fluorogenic TaqMan[®] probe and primers for β1, custom-designed TaqMan[®] probe and primers for β1B (located in the retained segment of intron 3), and 1x TaqMan[®] Universal PCR Master Mix (Applied Biosystems). PCR efficiency of the β1 and β1B fluorescent probes was estimated at ~98%. After 2 minutes at 50°C and 10 minutes at 95°C, 40 cycles of amplification were performed with the ABI PRISM 7900HT Sequence Detection System (Applied Biosystems). Data were collected with instrument spectral compensation by Applied Biosystems SDS 2.1 software and analyzed with the threshold cycle (Ct) relative-quantification method.²³

Fluorescence signals were normalized to the housekeeping gene hypoxanthine phosphoribosyl transferase 1 (*HPRT*). For each sample, $\beta 1$ and $\beta 1B$ transcripts were quantified in duplicate. The values were averaged and then used for the $2^{-\Delta Ct} \times 100$ calculation, where $2^{-\Delta Ct}$ corresponds to expression relative to *HPRT*. Primer and probe sequences are listed in Table 3:

Table 3.: Sequence of oligonucleotide primers for quantitative PCR

Gene isoform	GenBank accession No.	Target Exons	Forward primer	Reverse primer	Probe
<i>SCN1B</i> (transcript isoform $\beta 1$)	NM 001037	3-4	TaqMan® Gene Expression Assay Hs00168897_m1		
<i>SCN1B</i> (transcript isoform $\beta 1B$)	NM 199037	3A	CCACCGGAG- AGCCAGAT	GCCTGTCCT- GTCCACTGC	CTGCCATCT- GTCCCTCC
<i>HPRT1</i>	NM 000194	6-7	TaqMan® Gene Expression Assay Hs99999909_m1		

Generation of expression vectors

Full-length human $\beta 1$ cDNA (GenBank accession No. NM 001037) subcloned into a bicistronic vector also carrying the cDNA for enhanced green fluorescent protein (pEGFP-IRES, BD Biosciences-Clontech) was supplied by Dr. Al George (Vanderbilt University, Nashville, TN). Full-length human $\beta 1B$ cDNA (GenBank accession No. NM 199037) was cloned from human ventricular mRNA, supplied by Dr. Katherine Murray (Vanderbilt University). The $\beta 1B$ cDNA was subcloned into a pEGFP-IRES vector (BD Biosciences-Clontech). Mutant constructs were prepared using the QuikChange II XL Site-Directed Mutagenesis Kit (Stratagene) according to the manufacturer's instructions. The inserts were subsequently sequenced to ensure that there was no other mutation besides the intended one.

Transient transfection in CHO cells

For functional analysis, cultured Chinese Hamster Ovary (CHO) cells were transiently transfected with the constructs described above using FuGENE6 (Roche Applied Science). Constructs encoding $\beta 1$ - or $\beta 1B$ -subunits (1 μ g, unless otherwise specified) were cotransfected with the pBK-CMV vector (1 μ g, Stratagene) encoding *SCN5A* (GenBank accession No. NM 000335), supplied by Dr. Al George. To study dominant negative effects, mutant $\beta 1$ or $\beta 1B$ construct (0.5 μ g or 1 μ g) was cotransfected with the same amount of WT $\beta 1$ or $\beta 1B$ -subunit construct and subcloned into a bicistronic vector also carrying cDNA for red fluorescent protein from *Discosoma* version T3 (pDsRed T3-IRES, supplied by Dr. Al George), along with *SCN5A* (1 μ g). When *SCN5A* was transfected without β -subunits, the plasmid encoding the enhanced green fluorescent protein (pEGFP-IRES, BD Biosciences-Clontech) with no β -subunit insert was cotransfected. Cells were grown for 48 hours after transfection before study.

Electrophysiology

Cells displaying green fluorescence were chosen for study; in experiments with transfection of both WT and mutant β -subunits, cells displaying both green and red fluorescence were chosen. Sodium currents were measured at room temperature using the whole-cell configuration of the patch-clamp technique with an Axopatch 200B amplifier (Molecular Devices). The extracellular bath solution contained (in mmol/L): NaCl 145, KCl 4.0, MgCl₂ 1.0, CaCl₂ 1.8, glucose 10, HEPES 10, pH 7.4 (NaOH). Patch pipettes (~1.5 M Ω) contained (in mmol/L): NaF 10, CsF 110, CsCl 20, EGTA 10, and HEPES 10, pH 7.4 (CsOH). Currents were filtered at 5 kHz and digitized at 50 kHz. Cell capacitance and series resistance were compensated for by at least 80%. Voltage control, data acquisition, and analysis were accomplished using pClamp9.2 and Clampfit 9.2 software (Molecular Devices).

To study channel activation, cells were held at -120 mV, and currents were elicited with 50 ms depolarizing pulses from -80 to 60 mV in 10 mV increments. The voltage dependence of inactivation was studied using 500 ms prepulses from -120 to -20 mV in 10 mV increments followed by a test pulse to -20 mV. Recovery from inactivation was assessed by first inactivating channels using a 50-ms conditioning pulse to -20 mV from a holding potential of -120 mV, followed by a varying recovery duration, and a 10-ms test pulse to -20mV. The voltage-clamp protocols are shown in the figures. All currents were normalized to cell capacitance. Voltage-dependence of (in)activation was determined by fitting a Boltzmann function ($y=[1+\exp\{(V-V_{1/2})/k\}]^{-1}$), yielding the voltage required to achieve half-maximal conductance (activation) or channel availability (inactivation) ($V_{1/2}$) and slope factor (k). The time constants of recovery from inactivation were determined using a double-exponential function ($y=A_f\{1-\exp(-t/\tau_f)\}+A_s\{1-\exp(-t/\tau_s)\}$), where τ_f and τ_s are the time constants of fast and slow components, and A_f and A_s are the fractions of the fast and slow components.

Statistical analysis

Electrophysiological data are expressed as mean \pm SEM. Gene expression data are expressed as median \pm MAD (median absolute deviation). All statistical analyses were conducted with SPSS, version 12.0. To test for significant differences among groups, unpaired t -test or ANOVA was used. The level of statistical significance was $P<0.05$.

6.3 Results

Mutation analysis and clinical data

We screened 282 probands with Brugada syndrome and 44 with conduction disease for mutations in exons 1–5 of *SCN1B* encoding the β 1-subunit and in exon 3A, retained in the β 1B transcript (Figure 1, A and B). *SCN5A* coding region mutations had been previously excluded in all 326 subjects. Three variants were identified in probands and family members (Figure 2A). These variants were absent in 1,404 population controls.

A missense mutation, c.259G→C (Figure 2B) in exon 3 resulting in p.Glu87Gln within the extracellular immunoglobulin loop of the protein (Figure 1C), was identified in a Turkish kindred affected by conduction disease (family 1, Figure 2A). Alignment of the β 1-subunit amino acid sequence from multiple species demonstrated that Glu87 is highly conserved, supporting the importance of glutamate at this position (Figure 2C). The proband was a 50-year-old white Turkish female (II-1) who presented with palpitations and dizziness. Physical examination and echocardiography were normal, and her ECG showed complete left bundle branch block. A clinical electrophysiological study revealed a prolonged His-ventricle interval of 80 ms and inducible atrioventricular nodal reentrant tachycardia; complete atrioventricular block occurred following atrial programmed stimulation and during induced tachycardia. A dual-chamber pacemaker was implanted with resolution of symptoms. The same mutation was found in her brother (II-3), who had bifascicular block (right bundle branch block and left anterior hemiblock) and her mother (I-2), who had a normal ECG. There was no family history of syncope, sudden cardiac death, or epilepsy.

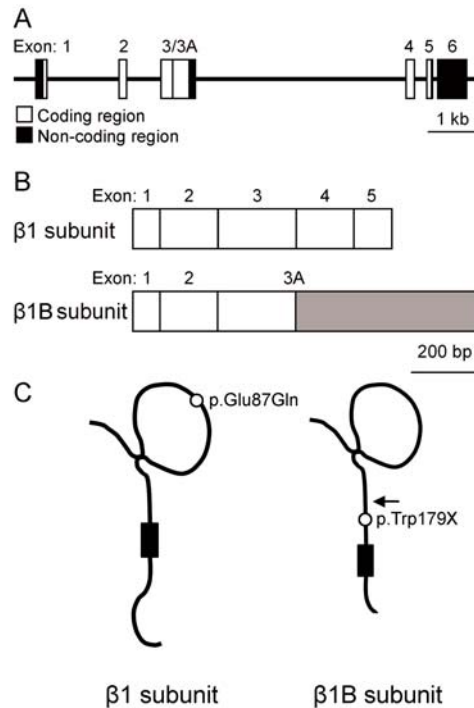


Figure 1: Structure of $\beta 1$ - and $\beta 1B$ -subunits. (A) Genomic structure of *SCN1B*. (B) Extension of exon 3 (c.208-458) into intron 3 creating a novel 3' end of the transcript (exon 3A, c.208-978), which generates an alternate transcript encoding $\beta 1B$. The gray region indicates the unique sequence of exon 3A. (C) Predicted topology of $\beta 1$ and $\beta 1B$. The $\beta 1B$ protein has unique juxtamembrane, transmembrane, and intracellular domains. The arrow indicates the initial amino acid of the $\beta 1B$ specific segment. Circles indicate the location of the mutations.

A nonsense mutation, c.536G→A in exon 3A (Figure, 1B and 2D), was identified in a French kindred affected with Brugada syndrome and conduction disease (family 2, Figure 2A). This mutation results in p.Trp179X and is predicted to generate a prematurely truncated protein lacking the membrane-spanning segment and intracellular portion of the protein (Figure 1C). The proband was a 53-year-old white male (II-4) who presented with chest pain. Physical examination, echocardiography, and coronary angiography were normal. His ECG showed ST-segment elevation typical of Brugada syndrome and conduction abnormalities (prolonged PR interval of 220 ms and left anterior hemiblock, Figure 2E).²⁴ Ventricular fibrillation was induced by programmed electrical stimulation in basal state (in absence of drugs). The same mutation was detected in his brother (II-1), nephew (III-1), and sister (II-2). The brother had no palpitations or history of syncope. His baseline ECG showed left anterior hemiblock and minor ST-segment elevation suggestive of Brugada syndrome at baseline (type II saddle back abnormality²⁴); with flecainide challenge, the ST segment elevation was further exaggerated, but did not meet criteria for a diagnostic (type I) pattern. The nephew had right bundle branch block and type II Brugada syndrome ECG after flecainide challenge and the sister had a normal ECG and a negative flecainide test. There was no family history of tachyarrhythmias, syncope, sudden cardiac death, or epilepsy.

A different nonsense mutation, c.537G→A in exon 3A (Figure 2D), resulting in p.Trp179X, affecting the same codon as in family 2, was identified in a Dutch kindred (family 3, Figure 2A). The proband was a 17-year-old white female (II-1). Physical examination and echocardiography were normal, and a flecainide test for Brugada syndrome was negative. Her ECG showed right bundle branch block and prolonged PR interval of 196 ms (normal upper limit in teenagers: 180 ms).²⁵ The same mutation was found in her father (I-1), with normal ECG and negative flecainide test. The family history was negative for syncope, sudden cardiac death, or epilepsy.

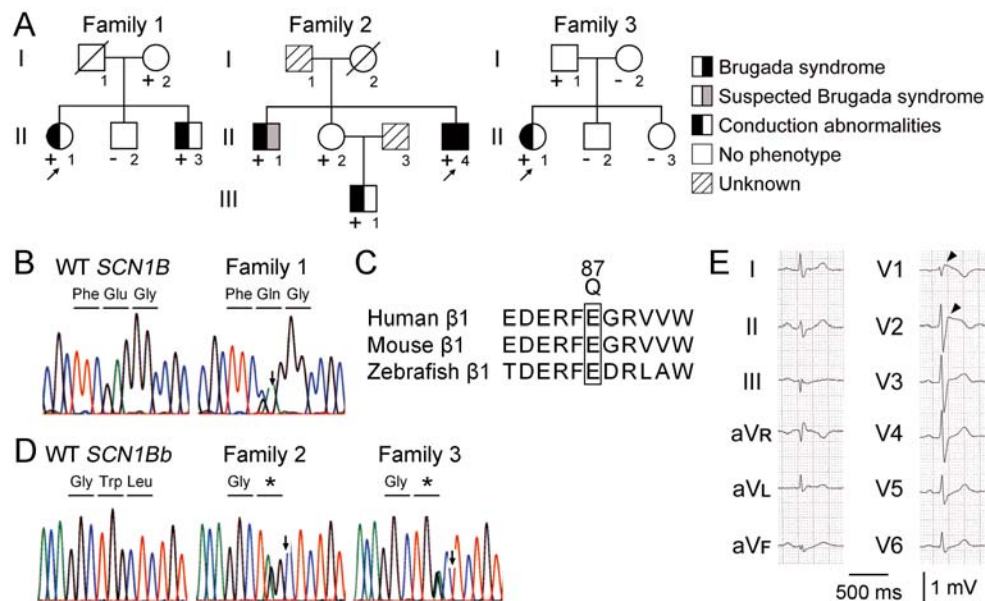


Figure 2: *SCN1B* mutations found in patients with Brugada syndrome and conduction disease. (A) Pedigrees and phenotypes of the families affected by Brugada syndrome and/or conduction disease. Individuals carrying the mutation are indicated (+). Individuals tested negative for the mutation are indicated (-). Individuals I-1 from family 1, and I-1 and II-3 from family 2 did not undergo genetic testing. Arrows indicate probands. (B) The c.259G→C mutation in *SCN1B* resulting in p.Glu87Gln found in family 1. (C) Alignment of $\beta 1$ across species showing the high conservation of Glu87. (D) The c.536G→A (middle) and c.537G→A (right) mutations in exon 3A of $\beta 1B$ both resulting in p.Trp179X found in families 2 and 3, respectively. (E) Twelve-lead ECG from the proband of family 2 (II-4). The arrowheads indicate ST-segment elevation typical of Brugada syndrome

$\beta 1$ and $\beta 1B$ transcript expression

To confirm and extend previous reports that $\beta 1B$ is expressed in brain, heart, skeletal muscle and other organs,¹⁹ we used quantitative real-time PCR in non-diseased human heart. Both $\beta 1$ and $\beta 1B$ transcripts were detected in right and left ventricles and in Purkinje fibers (Figure 3). The $\beta 1$ transcript level was higher in Purkinje fibers (which make up the conduction system in the ventricle) than left- (2.4-fold, $P < 0.05$) and right- (1.6-fold, $P = \text{NS}$) ventricular free wall. $\beta 1B$ transcript levels showed an even greater difference: Purkinje fibers versus left- (4.8-fold, $P < 0.001$) and right- (3.7-fold, $P < 0.001$) ventricular free wall. Levels of both transcripts were also slightly (but not statistically significantly) higher in right- versus left-ventricular free wall (1.5-fold and 1.3 fold for $\beta 1$ and $\beta 1B$ transcripts, respectively).

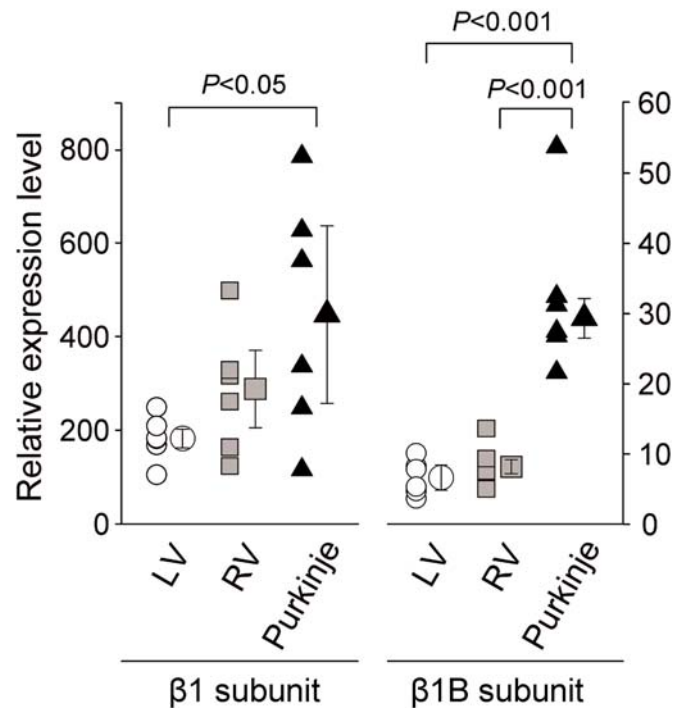


Figure 3: Expression profile of $\beta 1$ and $\beta 1B$ transcripts in non-diseased human ventricular tissue as determined by quantitative RT-PCR. Relative expression levels of the $\beta 1$ and $\beta 1B$ subunits are presented, normalized to those of *HPRT* in left ventricle (LV, circles), right ventricle (RV, squares), and Purkinje fibers (triangles). Tissues for each group were collected from 6 human donors (non-diseased hearts, $n=6$). Data points indicate the average of two measurements in each tissue sample. Larger symbols and error bars indicate median \pm MAD for all samples.

Cellular electrophysiology

The effects of mutant and WT $\beta 1$ and $\beta 1B$ variants on $Na_v1.5$ sodium current were assessed using the whole-cell patch-clamp technique in transfected CHO cells. As described in the methods, bicistronic expression vectors encoding a reporter (GFP or DsRed) with or without β -subunits were cotransfected with expression vector encoding $Na_v1.5$. Currents were compared in cells transfected with *SCN5A* alone or *SCN5A* plus WT, mutant, or both β -subunits.

p.Trp179X. Figure 4A shows representative current traces in cells expressing $Na_v1.5$ alone, and $Na_v1.5$ plus WT or mutant $\beta 1B$ (*p.Trp179X* $\beta 1B$) or their combination; current densities at -30 mV are summarized in Figure 4B. Coexpression of $Na_v1.5$ with WT $\beta 1B$ significantly increased sodium current density over $Na_v1.5$ alone, by 69%, while currents recorded with *p.Trp179X* $\beta 1B$ coexpression were no different from $Na_v1.5$ alone. Similarly, while coexpression of WT subunit with $Na_v1.5$ shifted the voltage-dependence of both activation and inactivation to more negative potentials compared to $Na_v1.5$ alone, no such shift was observed with the mutant (Figure 4C and Table 4). This result indicates that while WT $\beta 1B$ modulates $Na_v1.5$ gating (in a fashion similar to WT $\beta 1$; see below), the mutant exerts no such effect. Coexpression of WT or mutant $\beta 1B$ with $Na_v1.5$ did not alter recovery from inactivation (Figure 4D and Table 4).

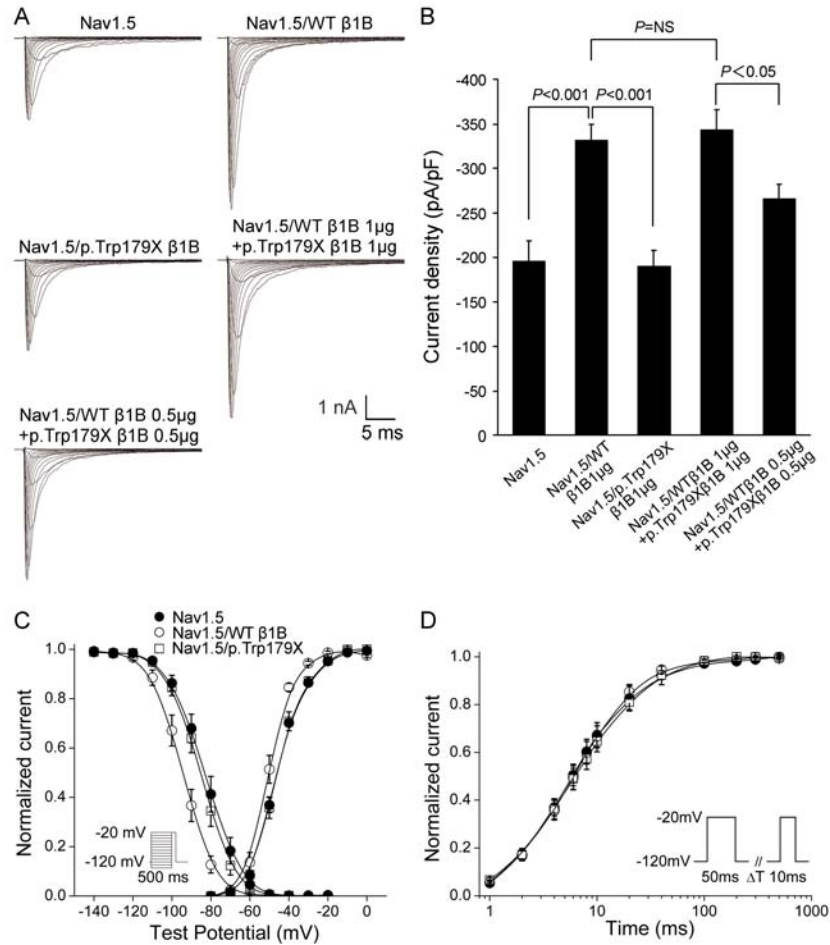


Figure 4: Electrophysiological characteristics of the p.Trp179X β1B mutant. (A) Representative traces of sodium current demonstrating an increase in sodium current with wild-type (WT) but not mutant subunit. (B) Sodium current density at -30 mV for Nav_v1.5 alone (n=29), Nav_v1.5 coexpressed with WT β1B (n= 28), Nav_v1.5 coexpressed with p.Trp179X β1B (n=18), Nav_v1.5 coexpressed with WT β1B + p.Trp179X β1B (1 μg of each, n=14), and Nav_v1.5 coexpressed with WT β1B + p.Trp179X β1B (0.5 μg of each, n=10). (C) Voltage dependence of activation and inactivation. Filled circles, open circles, and squares indicate Nav_v1.5 alone, Nav_v1.5 coexpressed with WT β1B, and Nav_v1.5 coexpressed with p.Trp179X β1B, respectively. The pulse protocol used to study the voltage dependence of inactivation is shown in the inset. (D) Recovery from steady-state inactivation. Biophysical properties are provided in Table 4.

To examine whether expression of the mutant influences the effect of WT β 1B on $\text{Na}_V1.5$ - (e.g., to produce a dominant negative action), cells were transfected with $\text{Na}_V1.5$ and varying amounts of WT and p.Trp179X β 1B. Figure 4B shows that the sodium current increase of $\text{Na}_V1.5$ alone recorded with transfection of 1 μg of both β 1B-subunit constructs was identical to the increase with that of 1 μg of WT β 1B. In addition, the increase in sodium current recorded with transfection of 0.5 μg of both β 1B-subunit constructs was 51% of that with 1 μg of β 1B alone. These data indicate that p.Trp179X β 1B does not exert a dominant negative effect on WT β 1B function, and further support the finding that the mutant, unlike WT, does not affect sodium channel function.

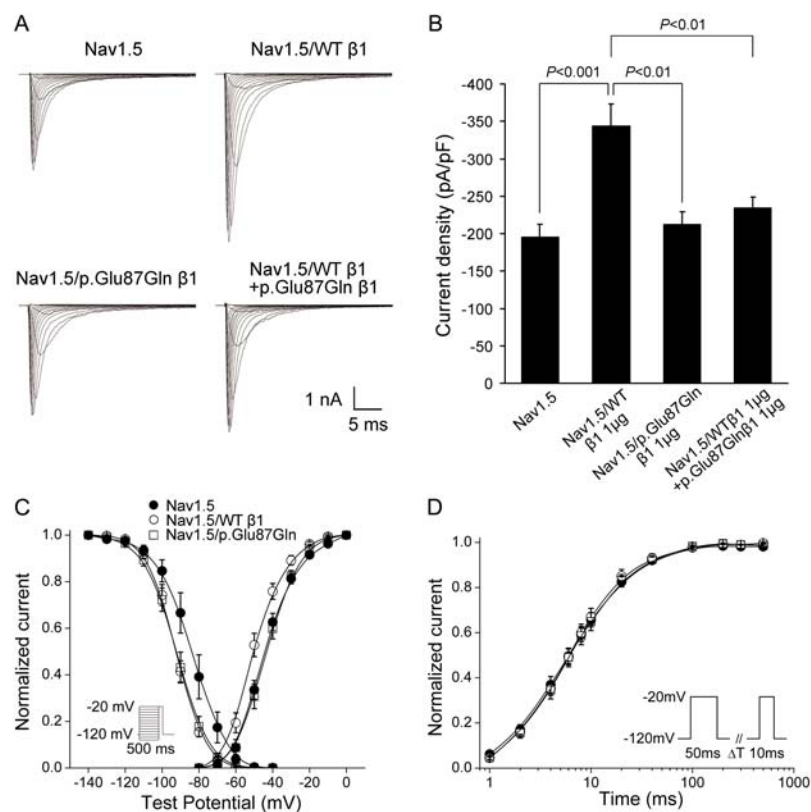


Figure 5: Electrophysiological characteristics of the p.Glu87Gln mutant. (A) Representative traces of sodium current. (B) Current density at -30 mV for $\text{Na}_V1.5$ alone ($n=13$), $\text{Na}_V1.5$ coexpressed with wild-type (WT) β 1 ($n=17$), $\text{Na}_V1.5$ coexpressed with p.Glu87Gln β 1 ($n=18$), and $\text{Na}_V1.5$ coexpressed with WT β 1 + p.Glu87Gln β 1 ($n=15$). (C) Voltage dependence of activation and inactivation. Filled circles, open circles, and squares indicate $\text{Na}_V1.5$ alone, $\text{Na}_V1.5$ coexpressed with WT β 1, and $\text{Na}_V1.5$ coexpressed with p.Glu87Gln β 1, respectively. (D) Recovery from steady-state inactivation. Biophysical properties are provided in Table 5.

Table 4.: Biophysical Parameters of WT and mutant $\beta 1B$

	Voltage dependence of activation			Voltage dependence of inactivation			Recovery from inactivation		
	$V_{1/2}$, mV	k, mV	N	$V_{1/2}$, mV	k, mV	N	τ_r , ms (amplitude, %)	τ_s , ms (amplitude, %)	N
Nav1.5	-46.2±1.0	7.1±0.4	29	-83.8±1.8	7.6±0.2	17	7.7±1.1 (87.2±1.1)	56.4±9.8 (11.6±1.0)	12
Nav1.5 / WT $\beta 1B$	-50.6±0.7*	6.3±0.3	28	-94.2±1.3*	7.6±0.2	14	7.4±1.0 (86.5±1.2)	43.3±8.6 (13.1±1.1)	14
Nav1.5 / p.Trp179X $\beta 1B$	-46.3±1.3 [†]	6.5±0.4 [†]	18	-85.2±2.0 [†]	6.6±0.3	15	8.2±1.0 (91.8±1.1)	58.0±11.9 (7.8±1.0)	12

Values are shown as mean ± SEM; * $P < 0.01$ when comparing versus Nav1.5 alone; [†] $P < 0.01$ when comparing versus Nav1.5 / WT $\beta 1B$.

Table 5: Biophysical Parameters of WT and mutant $\beta 1$

	Voltage dependence of activation			Voltage dependence of inactivation			Recovery from inactivation		
	$V_{1/2}$, mV	k, mV	N	$V_{1/2}$, mV	k, mV	N	τ_r , ms (amplitude, %)	τ_s , ms (amplitude, %)	N
Nav1.5	-46.1±1.7	7.8±0.4	13	-85.1±3.2	7.3±0.5	12	8.2±1.2 (88.2±1.3)	52.4±7.9 (11.0±1.3)	9
Nav1.5 / WT $\beta 1$	-50.6±1.4*	7.3±0.4	17	-92.6±1.4*	6.4±0.2	12	7.5±1.1 (84.2±1.3)	43.1±4.6 (14.1±1.3)	13
Nav1.5 / p.Glu87Gln $\beta 1$	-44.9±1.4 [†]	7.7±0.4	13	-92.5±1.7*	6.8±0.2	12	7.7±1.1 (89.1±1.1)	52.0±9.5 (10.4±1.1)	10

Values are shown as mean ± SEM; * $P < 0.05$ when comparing versus Nav1.5 alone; [†] $P < 0.05$ when comparing versus Nav1.5 / WT $\beta 1$.

p.Glu87Gln. Figure 5A shows representative current traces of $\text{Na}_v1.5$ and $\text{Na}_v1.5$ coexpressed with WT and/or mutant $\beta 1$ (*p.Glu87Gln* $\beta 1$); current densities are summarized in Figure 5B. Co-expression of $\text{Na}_v1.5$ with WT $\beta 1$ significantly increased sodium current density at -30 mV, by 76%, while coexpression with mutant $\beta 1$ (*p.Glu87Gln* $\beta 1$) did not increase the sodium current. The increase in sodium current recorded with coexpression of $\text{Na}_v1.5$ and $1 \mu\text{g}$ of both WT and *p.Glu87Gln* $\beta 1$ (+20%) was markedly smaller than the increase with coexpression of $\text{Na}_v1.5$ with $1 \mu\text{g}$ WT $\beta 1$ alone (+76%), indicating that this mutant exerts a dominant negative effect on WT $\beta 1$ function. Figure 5C shows that WT $\beta 1$ produced negative shifts in the voltage dependence of $\text{Na}_v1.5$ activation and inactivation similar to those observed with WT $\beta 1\text{B}$. *p.Glu87Gln* $\beta 1$ shifted the voltage dependence of inactivation to negative potentials (similar to WT), but did not alter the voltage dependence of activation (Table 5). Coexpression of WT or mutant $\beta 1$ with $\text{Na}_v1.5$ did not alter recovery from inactivation (Figure 5D, Table 5).

Since Glu87 is located in a region of the protein common to both $\beta 1$ and $\beta 1\text{B}$, we also studied the effects of *p.Glu87Gln* $\beta 1\text{B}$ on $\text{Na}_v1.5$ current properties (Figure 6, Table 6). While WT $\beta 1\text{B}$ increased $\text{Na}_v1.5$ current by 69% (Figure 4), *p.Glu87Gln* $\beta 1\text{B}$ did not increase the sodium current compared with $\text{Na}_v1.5$ alone. Similarly, WT $\beta 1\text{B}$ produced a negative shift in voltage dependence of both activation and inactivation (Table 4), while *p.Glu87Gln* $\beta 1\text{B}$ shifted only the voltage dependence of inactivation compared to $\text{Na}_v1.5$ alone. As with the other β -subunit constructs studied, there was no change in recovery from inactivation. Thus, the effects of *p.Glu87Gln* were comparable in the $\beta 1$ and the $\beta 1\text{B}$ backbones.

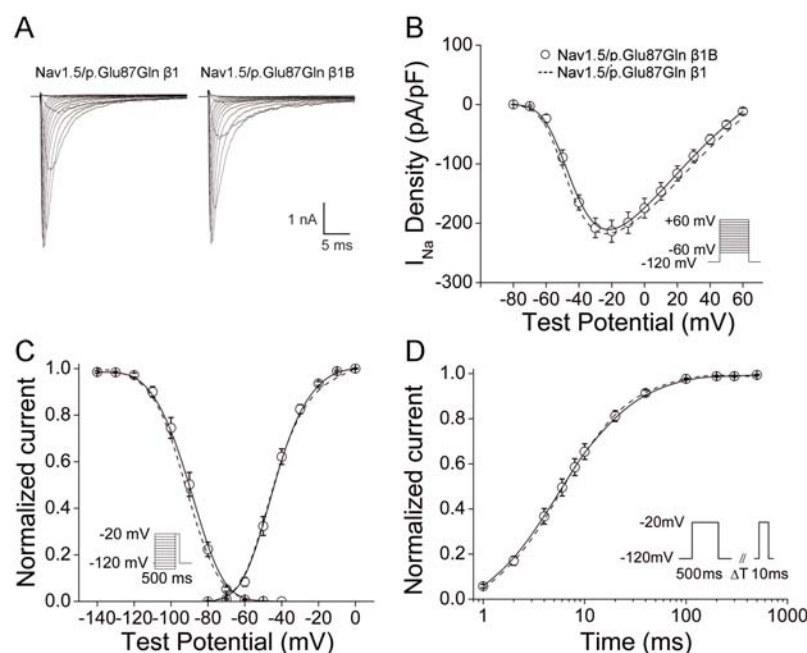


Figure 6: Comparison of *p.Glu87Gln* mutant function in $\beta 1$ - and $\beta 1\text{B}$ -subunits. (A) Representative traces of sodium current. (B) Current-voltage relationships for the *p.Glu87Gln* $\beta 1\text{B}$ -subunit (open circles, $n=15$). The dotted lines in panels B-D indicate data for the *p.Glu87Gln* $\beta 1$ -subunit shown in Figure 5. (C) Steady-state activation and inactivation. (D) Recovery from steady-state inactivation. Biophysical properties are provided in Table 6.

Table 6: Biophysical Parameters for p.Glu87Gln β 1

	Voltage dependence of activation			Voltage dependence of inactivation			Recovery from inactivation		
	$V_{1/2}$, mV	k, mV	N	$V_{1/2}$, mV	k, mV	N	τ_r , ms (%)	τ_s , ms (%)	N
Nav1.5	-46.2±1.0	7.1±0.4	29	-83.8±1.8	7.6±0.2	17	7.7±1.1 (87.2±1.1)	56.4±9.8 (11.6±1.0)	12
Nav1.5/WT β 1B	-50.6±0.7*	6.3±0.3	28	-94.2±1.3*	7.6±0.2	14	7.4±1.0 (86.5±1.2)	43.3±8.6 (13.1±1.1)	14
Nav1.5/p.Glu87Gln β 1B	-44.2±0.6 [†]	8.2±0.4	15	-90.6±0.8*	6.7±0.2	12	7.4±1.0 (87.6±1.1)	48.9±4.1 (11.5±1.1)	12
Nav1.5/p.Glu87Gln β 1	-44.9±1.4	7.7±0.4	13	-92.3±2.1*	6.8±0.2	9	7.7±1.1 (89.1±1.1)	52.0±9.5 (10.4±1.1)	10

Values are shown as mean ± SEM; * P<0.01 when comparing versus Nav_v1.5 alone; [†] P<0.01 when comparing versus Nav_v1.5 / WT β 1B. Data for Nav_v1.5, Nav_v1.5/WT β 1B, and Nav_v1.5/p.Glu87Gln β 1 are also shown in Tables 4 and 5.

6.4 Discussion

In this study we provide what we believe to be the first report of mutations in *SCN1B* sequences encoding the $\beta 1$ and $\beta 1B$ transcript variants in patients with conduction disease and/or Brugada syndrome. Further, we provide new data indicating that $\beta 1$ and $\beta 1B$ transcripts in the heart vary by region; greater expression in Purkinje fibers is consistent with the conduction system phenotype we describe in mutation carrier patients. Finally, we demonstrate that the $\beta 1$ and $\beta 1B$ variants modulate function of the major cardiac sodium channel α -subunit $Na_v1.5$, and that the identified *SCN1B* mutations blunt or inhibit this effect.

The three mutations were identified in three probands with conduction disease and/or Brugada syndrome as well as in other family members with or without these arrhythmia phenotypes. Formal linkage analysis was not possible because the families are too small and penetrance is incomplete. Thus, evidence in support of disease causality of these mutations (beyond their identification in subjects with clinical phenotypes) includes the findings that both $\beta 1$ and $\beta 1B$ transcripts are expressed in heart and that the mutant subunits (p.Glu87Gln $\beta 1$, p.Glu87Gln $\beta 1B$ and p.Trp179X $\beta 1B$) did not increase $Na_v1.5$ currents in heterologous expression experiments, while WT $\beta 1$ and $\beta 1B$ did. Incomplete penetrance, a well-recognized feature of the monogenic arrhythmia syndromes,^{12,26} was observed. For *SCN5A* mutations linked to Brugada syndrome, penetrance as low as 12.5% has been described.²⁷ A role for sex, age and genetic modifiers (e.g., common polymorphisms) is suspected,^{5,28,29} but the mechanisms for this common clinical finding remain poorly understood.

Two types of mutations were identified. The c.536G→A and c.537G→A mutations in exon 3A both result in a stop codon at position 179, predicted to generate a $\beta 1B$ protein lacking the transmembrane and cytoplasmic domains and thus unable to integrate into the sarcolemma and to associate with $Na_v1.5$. Thus, the *a priori* assumption is that a mutation such as this will cause disease by simple haploinsufficiency. The electrophysiologic data support this idea, since coexpression of p.Trp179X $\beta 1B$ failed to increase $Na_v1.5$ current and did not modulate the effect of the WT $\beta 1B$ protein. Furthermore, the voltage-dependencies of activation and inactivation of $Na_v1.5$ coexpressed with p.Trp179X $\beta 1B$ were the same as those for $Na_v1.5$ alone, in contrast to the shifts observed with WT $\beta 1B$.

On the other hand, the c.259G→C mutation leads to an amino acid substitution (p.Glu87Gln) within the extracellular domain of the protein. The electrophysiological data demonstrate that the mutant subunit did modulate $Na_v1.5$ gating (shift in the voltage dependence of inactivation, in either the $\beta 1$ or $\beta 1B$ background), supporting the idea that it associates with $Na_v1.5$ at the cell surface. In addition, in contrast to the p.Trp179X $\beta 1B$, p.Glu87Gln did exert a dominant-negative effect on the WT subunit. Thus, the three mutations lead to a decrease in $Na_v1.5$ current, through somewhat different mechanisms. This reduction of current is consistent with the conduction disease and Brugada syndrome phenotypes of the patients.

Normal impulse propagation in the atria, ventricles and Purkinje network is critically dependent on normal sodium channel function. Dysfunction of the sodium channel leads to conduction delay and loss-of-function mutations in *SCN5A* have been described in "pure" conduction disease.^{1,3} Thus, our finding of *SCN1B* mutations associated with reduced sodium current in patients with conduction disease is consistent with previous studies of the mechanism of this disorder. The preferential expression of the $\beta 1$ and $\beta 1B$ transcripts in human Purkinje fibers further supports the prominent conduction delay seen as part of the clinical phenotypes.

Loss-of-function mutations in *SCN5A* were the first reported cause of the Brugada syndrome.⁴ These mutations reduce sodium current by reducing $\text{Na}_v1.5$ cell surface expression and/or altering gating.^{4,5,30} A common view is that in epicardial cells, this reduction in sodium current produces marked action potential shortening, attributed to an “unopposed” early transient outward potassium current. By contrast, reduction of sodium current in endocardial cells is thought to produce only modest action potential shortening. The resultant increased heterogeneity of repolarization predisposes to rapid reentry resulting in ventricular fibrillation.^{4,31} A common feature in Brugada syndrome – consistent with reduced sodium current – is slowed conduction.^{32,33} Indeed, an alternate proposed mechanism suggests that the characteristic right precordial ST-segment elevation on the ECG and initiation of arrhythmias is attributable primarily to right-ventricular outflow tract conduction delay.³³ The trend to higher expression levels of $\beta1B$ in right ventricle may thus contribute to the Brugada syndrome phenotype.

This idea is further supported by functional studies of the *GPD1L* mutation linked to Brugada syndrome in a single large kindred: coexpression of mutant *GPD1L* with $\text{Na}_v1.5$ was reported to decrease sodium current, consistent with the loss-of-function mutations in *SCN5A* itself as a cause for Brugada syndrome.¹² In principle, reduction in L-type calcium current might also produce differential effects in epicardial and endocardial sites, and thus cause the Brugada syndrome; rare kindreds with this mechanism have now been described.¹⁴

Conduction disease was observed in families 1 and 3, while in family 2, mutation carriers presented either solely with conduction disease or conduction disease in combination with ECGs typical of Brugada syndrome. This phenomenon of overlapping clinical phenotypes is common in individuals with *SCN5A* mutations leading to loss of sodium channel function,^{6,8} and conversely *in vitro* electrophysiologic analysis of *SCN5A* mutations linked to Brugada syndrome or isolated conduction disease consistently reveals loss of $\text{Na}_v1.5$ channel function.^{3,4} Indeed, a single mutation segregating in a given family can lead to conduction disease in some family members and Brugada syndrome in others.^{6,8} What determines the ultimate phenotype – Brugada syndrome versus isolated conduction disease – is unknown. Sex, age, and genetic modifiers (e.g., common polymorphisms) have been proposed as modulators of the clinical phenotypes.^{5,28,29}

The reported effects of $\beta1$ on $\text{Na}_v1.5$ channels are controversial.³⁴ Some groups have reported that $\beta1$ increases $\text{Na}_v1.5$ currents with or without affecting voltage dependence or channel kinetics, while others have reported no effect of $\beta1$ on $\text{Na}_v1.5$ current.^{20,35–39} The $\beta1B$ variant has to date only been studied in coexpression studies with the neuronal sodium channel $\text{Na}_v1.2$ (encoded by *SCN2A*) where it was shown to increase sodium current and cause a small negative shift in voltage dependence of activation.¹⁹ In our experiments, WT $\beta1$ and $\beta1B$ had similar effects on $\text{Na}_v1.5$ current: both increased sodium currents and led to hyperpolarizing (negative) shifts in voltage-dependence of activation and inactivation.

Not only were the effects of the WT β -subunits on $\text{Na}_v1.5$ current similar, but the effects of the p.Glu87Gln mutation in the $\beta1$ background (p.Glu87Gln $\beta1$) were also similar to those in the $\beta1B$ background (p.Glu87Gln $\beta1B$). Although the $\beta1$ and $\beta1B$ variants share the same topology (an N-terminal extracellular immunoglobulin domain, a transmembrane domain, and a C-terminal cytoplasmic domain), their sequence identity is limited to the extracellular immunoglobulin domain; the C-terminal half of $\beta1B$, residues 150–268, has only ~17% amino acid sequence identity with $\beta1$.¹⁹ Taken together, the data suggest that the molecular determinants of $\beta1$ and $\beta1B$ modulation of $\text{Na}_v1.5$ cell-surface expression and gating likely reside in the

extracellular immunoglobulin domain. This is in line with previous studies of skeletal muscle ($\text{Na}_v1.4$ encoded by *SCN4A*) and neuronal ($\text{Na}_v1.2$) sodium channel α -subunits that have shown that deletion of the intracellular domain of the $\beta 1$ -subunit has no effect on its modulation of α -subunit function, whereas deletions within the extracellular domain block modulation.⁴⁰⁻⁴² Alternatively, specific residues may not be as important as preservation of overall structural motifs, as suggested by the data of Zimmer and Benndorf who reported that the $\beta 1$ -subunit modulates $\text{Na}_v1.5$ via the membrane anchor plus additional intracellular or extracellular regions.⁴³

In addition to modulating sodium channel α -subunit expression and function, other roles have been suggested for β -subunits: these include acting as adhesion molecules or as participants in signal transduction.^{17,34} The different transmembrane and C-terminal domains of $\beta 1$ and $\beta 1B$ might therefore lead to participation in different signaling pathways. For instance, phosphorylation of the tyrosine at position 181 of the $\beta 1$ C-terminus regulates its interaction with ankyrin-G,⁴⁴ which is thought to be critical for ankyrin-G localization within cardiomyocytes (intercalated discs versus T-tubules). $\beta 1B$ lacks this tyrosine in its C-terminal domain, so a role for $\beta 1B$ as a modulator of this function seems less likely.

Mutations in *SCN1B* have been previously reported in generalized epilepsy with febrile seizures plus,⁴⁵ and $\beta 1$ null mice exhibit a severe seizure disorder and die at age ~3 weeks.⁴⁶ In addition, these mice exhibit bradycardia and prolonged rate-corrected QT intervals.⁴⁷ These changes suggest that $\beta 1$ plays an important role in the murine heart, although it is possible that the changes are a consequence of the severe overall developmental phenotype in this model.⁴⁶ To our knowledge, defects in cardiac function have not been investigated in *SCN1B* mutation carriers presenting with epilepsy.^{34,48} Conversely, we have observed no neurological phenotype in our patients. Four *SCN1B* mutations have been linked to epilepsy to date,^{45,48,49} all of which localize to the extracellular immunoglobulin-like fold of the protein, as does the p.Glu87Gln mutation reported here. One additional possible link between the cardiac and neurological phenotypes associated with $\beta 1$ mutations is the syndrome of Sudden Unexpected Death in Epilepsy (SUDEP),⁵⁰ where a role for cardiac bradyarrhythmias has been proposed.⁵¹

A conventional heterologous mammalian expression system was used for functional assessment of the mutations. The environment in this approach is different from that in native cardiomyocytes and other proteins known to associate with the sodium channel complex, such as other β -subunits, are generally absent. Despite these limitations, the *in vitro* characteristics of the mutations were concordant with the phenotype observed in the patients and in combination with the genetic data presented, supports the disease causality of the mutations.

In summary, we have for the first time to our knowledge identified *SCN1B* mutations in families with conduction disease and Brugada syndrome. We have shown expression of the $\beta 1$ -subunit transcript and the alternate $\beta 1B$ -subunit transcript variant in human heart and demonstrated reduced $\text{Na}_v1.5$ sodium current as a result of loss or altered β -subunit modulation of $\text{Na}_v1.5$ current. These findings implicate *SCN1B* as a disease gene for human arrhythmia susceptibility.

Acknowledgements

We thank Leander Beekman, Peter van Tintelen, Arie O. Verkerk, Carol Ann Remme, Alfred George, Katherine Murray, Sabina Kupersmidt, Kai Liu, Sameer Chopra, Nathalie Gaborit, Satoru Komura, Mahmut Akyol and Moritz Sinner for their contributions to performing and/or analyzing this work and for helpful discussions. This work was supported by grants from the US National Institutes of Health (HL46681, HL65962, DMR), a Fondation Leducq Trans-Atlantic network of Excellence grant (05 CVD 01, Preventing Sudden Death), Netherlands Heart Foundation grant 2003T302 (AAMW), the Interuniversity Cardiology Institute of the Netherlands (project 27, AAMW), ANR grant 05-MRAR-028, GIS Institut des Maladies Rares grant (JJS), German Federal Ministry of Education and Research (BMBF) grants 01GI0204, 01GS0499, 01GI0204 and 01GR0103 (SK, AP, HEW), and Sumitomo Life Social Foundation grant (HW). The KORA platform is funded by the BMBF and by the State of Bavaria. Resequencing Coriell samples was performed by the J. Craig Venter Institute through the NHLBI Resequencing and Genotyping Program. We also thank Andras Varro (Department of Pharmacology and Pharmacotherapy, University of Szeged, Szeged, Hungary) for providing the human tissues. Dr. Bezzina is an Established Investigator of the Netherlands Heart Foundation (Grant 2005/T024).

Reference List

1. Tan, H. L. *et al.* A sodium-channel mutation causes isolated cardiac conduction disease. *Nature* **409**, 1043-1047 (2001).
2. Wang, Q. *et al.* SCN5A mutations associated with an inherited cardiac arrhythmia, long QT syndrome. *Cell* **80**, 805-811 (1995).
3. Schott, J. J. *et al.* Cardiac conduction defects associate with mutations in SCN5A. *Nat. Genet.* **23**, 20-21 (1999).
4. Chen, Q. *et al.* Genetic basis and molecular mechanism for idiopathic ventricular fibrillation. *Nature* **392**, 293-296 (1998).
5. Tan, H. L., Bezzina, C. R., Smits, J. P., Verkerk, A. O. & Wilde, A. A. Genetic control of sodium channel function. *Cardiovasc. Res.* **57**, 961-973 (2003).
6. Bezzina, C. *et al.* A single Na⁺ channel mutation causing both long-QT and Brugada syndromes. *Circ. Res.* **85**, 1206-1213 (1999).
7. Grant, A. O. *et al.* Long QT syndrome, Brugada syndrome, and conduction system disease are linked to a single sodium channel mutation. *J. Clin. Invest* **110**, 1201-1209 (2002).
8. Kyndt, F. *et al.* Novel SCN5A mutation leading either to isolated cardiac conduction defect or Brugada syndrome in a large French family. *Circulation* **104**, 3081-3086 (2001).
9. Remme, C. A. *et al.* Overlap syndrome of cardiac sodium channel disease in mice carrying the equivalent mutation of human SCN5A-1795insD. *Circulation* **114**, 2584-2594 (2006).
10. Valdivia, C. R. *et al.* A novel SCN5A arrhythmia mutation, M1766L, with expression defect rescued by mexiletine. *Cardiovasc. Res.* **55**, 279-289 (2002).
11. Shimizu, W., Aiba, T. & Kamakura, S. Mechanisms of disease: current understanding and future challenges in Brugada syndrome. *Nat. Clin. Pract. Cardiovasc. Med* **2**, 408-414 (2005).
12. London, B. *et al.* Mutation in glycerol-3-phosphate dehydrogenase 1 like gene (GPD1-L) decreases cardiac Na⁺ current and causes inherited arrhythmias. *Circulation* **116**, 2260-2268 (2007).
13. Koopmann, T. T. *et al.* Exclusion of multiple candidate genes and large genomic rearrangements in SCN5A in a Dutch Brugada syndrome cohort. *Heart Rhythm*. **4**, 752-755 (2007).

14. Antzelevitch, C. *et al.* Loss-of-function mutations in the cardiac calcium channel underlie a new clinical entity characterized by ST-segment elevation, short QT intervals, and sudden cardiac death. *Circulation* **115**, 442-449 (2007).
15. Moric, E. *et al.* The implications of genetic mutations in the sodium channel gene (SCN5A). *Europace*. **5**, 325-334 (2003).
16. Abriel, H. & Kass, R. S. Regulation of the voltage-gated cardiac sodium channel Nav1.5 by interacting proteins. *Trends Cardiovasc. Med.* **15**, 35-40 (2005).
17. Isom, L. L. Sodium channel beta subunits: anything but auxiliary. *Neuroscientist*. **7**, 42-54 (2001).
18. Kazen-Gillespie, K. A. *et al.* Cloning, localization, and functional expression of sodium channel beta1A subunits. *J. Biol. Chem.* **275**, 1079-1088 (2000).
19. Qin, N. *et al.* Molecular cloning and functional expression of the human sodium channel beta1B subunit, a novel splicing variant of the beta1 subunit. *Eur. J. Biochem.* **270**, 4762-4770 (2003).
20. Nuss, H. B., Chiamvimonvat, N., Perez-Garcia, M. T., Tomaselli, G. F. & Marban, E. Functional association of the beta 1 subunit with human cardiac (hH1) and rat skeletal muscle (μ 1) sodium channel alpha subunits expressed in *Xenopus* oocytes. *J. Gen. Physiol* **106**, 1171-1191 (1995).
21. Wichmann, H. E., Gieger, C. & Illig, T. KORA-gen—resource for population genetics, controls and a broad spectrum of disease phenotypes. *Gesundheitswesen* **67 Suppl 1**, S26-S30 (2005).
22. Gaborit, N. *et al.* Regional and tissue specific transcript signatures of ion channel genes in the non-diseased human heart. *J. Physiol* **582**, 675-693 (2007).
23. Livak, K. J. & Schmittgen, T. D. Analysis of relative gene expression data using real-time quantitative PCR and the 2(-Delta Delta C(T)) Method. *Methods* **25**, 402-408 (2001).
24. Wilde, A. A. *et al.* Proposed diagnostic criteria for the Brugada syndrome. *Eur Heart J* **23**, 1648-1654 (2002).
25. Dickinson, D. F. The normal ECG in childhood and adolescence. *Heart* **91**, 1626-1630 (2005).
26. Priori, S. G., Napolitano, C. & Schwartz, P. J. Low penetrance in the long-QT syndrome: clinical impact. *Circulation* **99**, 529-533 (1999).
27. Priori, S. G. *et al.* Clinical and genetic heterogeneity of right bundle branch block and ST-segment elevation syndrome: A prospective evaluation of 52 families. *Circulation* **102**, 2509-2515 (2000).
28. Bezzina, C. R. *et al.* Common Sodium Channel Promoter Haplotype in Asian Subjects Underlies Variability in Cardiac Conduction. *Circulation* **113**, 338-344 (2006).
29. Viswanathan, P. C., Benson, D. W. & Balsler, J. R. A common SCN5A polymorphism modulates the biophysical effects of an SCN5A mutation. *J. Clin. Invest* **111**, 341-346 (2003).
30. Baroudi, G. *et al.* Novel mechanism for Brugada syndrome: defective surface localization of an SCN5A mutant (R1432G). *Circ. Res.* **88**, E78-E83 (2001).
31. Yan, G. X. & Antzelevitch, C. Cellular basis for the Brugada syndrome and other mechanisms of arrhythmogenesis associated with ST-segment elevation. *Circulation* **100**, 1660-1666 (1999).
32. Antzelevitch, C. *et al.* Brugada syndrome: report of the second consensus conference: endorsed by the Heart Rhythm Society and the European Heart Rhythm Association. *Circulation* **111**, 659-670 (2005).
33. Meregalli, P. G., Wilde, A. A. & Tan, H. L. Pathophysiological mechanisms of Brugada syndrome: depolarization disorder, repolarization disorder, or more? *Cardiovasc. Res.* **67**, 367-378 (2005).
34. Meadows, L. S. & Isom, L. L. Sodium channels as macromolecular complexes: implications for inherited arrhythmia syndromes. *Cardiovasc. Res.* **67**, 448-458 (2005).
35. Fahmi, A. I. *et al.* The sodium channel beta-subunit SCN3b modulates the kinetics of SCN5a and is expressed heterogeneously in sheep heart. *J. Physiol* **537**, 693-700 (2001).

36. Johnson, D., Montpetit, M. L., Stocker, P. J. & Bennett, E. S. The sialic acid component of the beta1 subunit modulates voltage-gated sodium channel function. *J. Biol. Chem.* **279**, 44303-44310 (2004).
37. Ko, S. H., Lenkowski, P. W., Lee, H. C., Mounsey, J. P. & Patel, M. K. Modulation of Na(v)1.5 by beta1— and beta3-subunit co-expression in mammalian cells. *Pflugers Arch.* **449**, 403-412 (2005).
38. Makita, N., Bennett, P. B., Jr. & George, A. L., Jr. Voltage-gated Na⁺ channel beta 1 subunit mRNA expressed in adult human skeletal muscle, heart, and brain is encoded by a single gene. *J. Biol. Chem.* **269**, 7571-7578 (1994).
39. Qu, Y. *et al.* Modulation of cardiac Na⁺ channel expression in *Xenopus* oocytes by beta 1 subunits. *J. Biol. Chem.* **270**, 25696-25701 (1995).
40. Chen, C. & Cannon, S. C. Modulation of Na⁺ channel inactivation by the beta 1 subunit: a deletion analysis. *Pflugers Arch.* **431**, 186-195 (1995).
41. McCormick, K. A. *et al.* Molecular determinants of Na⁺ channel function in the extracellular domain of the beta1 subunit. *J. Biol. Chem.* **273**, 3954-3962 (1998).
42. McCormick, K. A., Srinivasan, J., White, K., Scheuer, T. & Catterall, W. A. The extracellular domain of the beta1 subunit is both necessary and sufficient for beta1-like modulation of sodium channel gating. *J. Biol. Chem.* **274**, 32638-32646 (1999).
43. Zimmer, T. & Benndorf, K. The human heart and rat brain IIA Na⁺ channels interact with different molecular regions of the beta1 subunit. *J. Gen. Physiol.* **120**, 887-895 (2002).
44. Malhotra, J. D., Thyagarajan, V., Chen, C. & Isom, L. L. Tyrosine-phosphorylated and nonphosphorylated sodium channel beta1 subunits are differentially localized in cardiac myocytes. *J. Biol. Chem.* **279**, 40748-40754 (2004).
45. Wallace, R. H. *et al.* Febrile seizures and generalized epilepsy associated with a mutation in the Na⁺-channel beta1 subunit gene SCN1B. *Nat. Genet.* **19**, 366-370 (1998).
46. Chen, C. *et al.* Mice lacking sodium channel beta1 subunits display defects in neuronal excitability, sodium channel expression, and nodal architecture. *J. Neurosci.* **24**, 4030-4042 (2004).
47. Lopez-Santiago, L. F. *et al.* Sodium channel Scn1b null mice exhibit prolonged QT and RR intervals. *J. Mol. Cell Cardiol.* **43**, 636-647 (2007).
48. Scheffer, I. E. *et al.* Temporal lobe epilepsy and GEFS+ phenotypes associated with SCN1B mutations. *Brain* **130**, 100-109 (2007).
49. Audenaert, D. *et al.* A deletion in SCN1B is associated with febrile seizures and early-onset absence epilepsy. *Neurology* **61**, 854-856 (2003).
50. Nashef, L., Hindocha, N. & Makoff, A. Risk factors in sudden death in epilepsy (SUDEP): the quest for mechanisms. *Epilepsia* **48**, 859-871 (2007).
51. Rugg-Gunn, F. J., Simister, R. J., Squirell, M., Holdright, D. R. & Duncan, J. S. Cardiac arrhythmias in focal epilepsy: a prospective long-term study. *Lancet* **364**, 2212-2219 (2004).